Enhancing optoelectronic properties of SiC-grown graphene by a surface layer of colloidal quantum dots

2D Materials

OPEN ACCESS

RECEIVED
12 April 2017

REVISED
26 May 2017

ACCEPTED FOR PUBLICATION
2 June 2017

PUBLISHED
19 June 2017

LETTER

Enhancing optoelectronic properties of SiC-grown graphene by a surface layer of colloidal quantum dots

Oleg Makarovsky[1], Lyudmila Turyanska[1,2], Nobuya Mori[3], Mark Greenaway[1,4], Laurence Eaves[1], Amalia Patané[1], Mark Fromhold[1], Samuel Lara-Avila[5], Sergey Kubatkin[5] and Rositsa Yakimova[6]

[1] School of Physics and Astronomy, The University of Nottingham, NG7 2RD, United Kingdom
[2] School of Chemistry, University of Lincoln, LN6 7DL, United Kingdom
[3] Division of Electrical, Electronic and Information Engineering, Graduate School of Engineering, Osaka University, Suita, Osaka 565-0871, Japan
[4] Department of Physics, Loughborough University, LE11 3TU, United Kingdom
[5] Department of Microtechnology and Nanoscience, Chalmers University of Technology, Göteborg, S-41296, Sweden
[6] Department of Physics, Chemistry and Biology, Linkoping University, S58183, Sweden

E-mail: Lyudmila.Turyanska@nottingham.ac.uk

Keywords: SiC-graphene, unipolar charge correlation, colloidal quantum dots, Monte Carlo simulations

Supplementary material for this article is available online

Abstract

We report a simultaneous increase of carrier concentration, mobility and photoresponsivity when SiC-grown graphene is decorated with a surface layer of colloidal PbS quantum dots, which act as electron donors. The charge on the ionised dots is spatially correlated with defect charges on the SiC-graphene interface, thus enhancing both electron carrier density and mobility. This charge-correlation model is supported by Monte Carlo simulations of electron transport and used to explain the unexpected 3-fold increase of mobility with increasing electron density. The enhanced carrier concentration and mobility give rise to Shubnikov-de Haas oscillations in the magnetoresistance, which provide an estimate of the electron cyclotron mass in graphene at high densities and Fermi energies up to 1.2 $\times$ 10^{13} cm^{-2} and 400 meV, respectively.

Although developments in graphene-based electronics have already led to a number of novel devices ranging from portable quantum Hall resistance standards [1, 2] to ultrasensitive photon detectors [3, 4], future commercialization of this technology is likely to require large area single layer graphene (SLG). Epitaxial graphene can be grown on a large scale by chemical vapour deposition (CVD) on Cu [5] or by thermal decomposition of the surface atomic layers of SiC [6]. However, both methods produce graphene with a significant concentration of unintentional dopants, which scatter the conduction electrons and reduce the carrier mobility [7] compared to exfoliated graphene, for which mobilities of ~100 000 cm^2 V^{-1} s^{-1} can be achieved [8].

The high temperature growth of graphene by thermal decomposition of SiC produces a phase which is thermodynamically stable [6], but with a high density of dangling bonds. Post-growth treatments, e.g. hydrogenation [7] or intercalation with different elements (e.g. Li, Ag, Si) [6, 9, 10] are routinely used to improve the carrier mobility by reducing the number of scattering centres [11]. An alternative strategy for controlling the electronic properties of graphene, including its photosensitivity, is to functionalise it chemically or combine it with nanomaterials.

Here we demonstrate that the electrical and optical properties of *n*-type graphene on SiC can be significantly enhanced by decorating the graphene surface with a layer of colloidal PbS quantum dots (QDs), which act as electron donors. This leads to a significant increase of the electron concentration in graphene from $n = 5.2 \times 10^{12}$ cm^{-2} to $n = 1.2 \times 10^{13}$ cm^{-2}, accompanied by a remarkable 3-fold enhancement of the low-temperature mobility, which we attribute to a reduction of elastic scattering due to a charge correlation effect. This enhancement of the electrical properties enables the observation of Shubnikov-de Haas (SdH) magnetoresistance oscillations and allows us to estimate the electron cyclotron mass in graphene up to Fermi energies of 400 meV above the Dirac point, significantly higher than those reported previously [12]. The presence of the PbS QDs, which are optically active in the near infrared spectral range, also produces a device with a strong photoresponsivity of up to $R = 10^5$ A W^{-1}. We explain our measurements in terms of the

transfer of electronic charge from the QDs to the graphene layer and of the spatial correlation of the charges in these two layers. Our Monte Carlo simulations of the electron transport in graphene provide additional support to this model. These results are relevant to the future exploitation of SiC-grown SLG in functional devices.

The SiC-grown graphene (SiC-SLG) [13, 14] was processed into Hall Bars with a channel width $w = 20$ μm and length $L = 100$ μm, as shown in figure 1(a). The electrical properties and photoresponse were measured firstly on control samples, i.e. pristine SiC graphene devices. The devices were then decorated with a layer of colloidal PbS QDs with an average PbS nanocrystal diameter of $d_{PbS} = 4.5$ nm. PbS QDs were synthesised in aqueous solution and were capped with a mixture of thioglycerol and 2,3-dimercaptopropanol (TGL) of length $l \approx 0.5$ nm (figure 1(b)) [15]. To achieve full coverage of the SLG, the QD solution with concentration of 10^{16} QDs ml^{-1} was drop-casted onto the graphene device and dried in vacuum at $P \sim 10^{-8}$ bar for 12 h. We note that once the QDs fully cover the graphene layer, any further increase in the thickness of the QD layer does not change significantly the properties of SLG. All electrical measurements were performed in a cryostat equipped with a superconducting magnet ($B \leqslant 14$ T) in the temperature range 2 K$< T <$ 250 K. We measured the photoresponse in vacuum at room temperature with excitation from a HeNe laser beam at $\lambda = 633$ nm and P up to 5×10^3 W m^{-2}.

The results of our Hall effect measurements of SLG with and without the QD layer are shown in the figure 1(c). The electrical properties of the pristine devices are typical of heavily doped SiC single-layer graphene. They have an almost temperature-independent electron concentration, $n = 5.2 \times 10^{12}$ cm^{-2}, and a Hall mobility which increases from $\mu = 720$ cm^{2}V^{-1}s^{-1} at $T = 250$ K to $\mu = 1000$ cm^{2}V^{-1}s^{-1} at $T = 2$ K. These graphene layers show no detectable photoresponse (figure 1(d)). Deposition of the QD layer leads to an increase of electron concentration to $n = 1.2 \times 10^{13}$ cm^{-2}, a value which remains roughly independent of temperature over a wide range from 2 K to 250 K, and to a significant increase in the Hall mobility, $\mu = 1600$ cm^{2}V^{-1}s^{-1} ($T = 250$ K) and 3000 cm^{2}V^{-1}s^{-1} ($T = 2$ K). In addition, the deposition of the QD layer induces a very strong photoresponsivity of up to $R = 10^5$ A W^{-1} (inset in figure 1(d)), not achieved previously in SiC-graphene, and is comparable to that reported for QD-decorated CVD SLG [3]. The photocurrent is proportional to the applied bias.

The high value of photoresponsivity can be understood in terms of the long lifetime, τ_{QD}, of photogenerated charge bound to the QDs, relative to the time, τ_d, taken for an electron to drift down the length of the graphene channel [16]. The photoresponsivity is $R = \alpha e\tau_{QD}/h\nu\tau_d$, where α is the optical absorbance of the PbS QDs [17] and $\tau_d = L^2/\mu V_s = 2 \times 10^{-7}$ s at $V_s = 0.2$ V. From the measured value of $R = 10^5$ A W^{-1}, we estimate $\tau_{QD} \approx 0.1$ s, comparable to the lifetime of holes reported in CVD graphene capped with similar QDs [16]. The photoresponsivity of QD-decorated graphene devices exhibits a power-law dependence of the type $\sim P^{-\alpha}$, where $\alpha = 0.9$ (inset in figure 1(d)), which was also observed previously [3, 16, 18]. The deviation from this power-law dependence at low incident powers is attributed to reduction of the signal-to-noise ratio.

The simultaneous increase of carrier concentration and mobility induced by the deposited QD layer is sufficient to observe a series of well-defined SdH oscillations in the low temperature magnetoresistance at magnetic fields, $B \gtrsim 7$ T, as shown in figures 1(c) and 2(a). Fourier analysis reveals that the oscillations, which are periodic in $1/B$, have a fundamental field, $B_f = 129$ T. Assuming a Landau valley and spin degeneracy, $g = 4$, we obtain an electron sheet density of $n_{SdH} = 4eB_f/h = 1.2 \times 10^{13}$ cm^{-2}, in close agreement with that obtained from the low field classical Hall effect.

The temperature dependence of the SdH oscillations (figure 2(a)) allows us to estimate the cyclotron effective mass of the electrons, m_c, up to electron concentrations and Fermi energy significantly higher than reported previously [12]. We fit the dependence of the SdH amplitude on T and B to the following relation [12, 19]:

$$R_{xx}(T, B) \sim T/\sinh(2\pi^2 k_B T m_c/\hbar eB). \quad (1)$$

Representative results are shown in figure 2(b) for $B = 13.4$ T (red) and $B = 9.8$ T (blue). We thereby estimate $m_c = 0.083 \pm 0.006 m_e$, where m_e is the free electron mass. For a linear band dispersion, $E = \hbar k v_F$, the electron cyclotron mass can be written as $m_c = \frac{E_F}{v_F^2}$. Then the Fermi velocity, v_F, and Fermi energy, E_F, are given by $v_F = \hbar\sqrt{\pi n}/m_c$ and $E_F = v_F\hbar\sqrt{\pi n}$, where n is the electron sheet density. We obtain $v_F = 0.86 \pm 0.06 \times 10^6$ m s^{-1}, which is in good agreement with that previously reported for exfoliated graphene [12] (green curve in the inset in figure 2(b)), but lower than that reported for SiC-grown graphene ($v_F = 1.02 \pm 0.01 \times 10^6$ m s^{-1}) [20, 21]. Our result confirms that the energy-wavevector dispersion of SLG remains linear up to electron concentrations of 10^{13} cm^{-2} and Fermi energies 400 meV. This suggests that the low values of mobility, typically observed in highly doped graphene, are not associated with the increase of SLG electron cyclotron mass at high Fermi energies.

We now consider the origin of the enhanced values for the carrier concentration and mobility in the QD-decorated graphene. The main mobility-limiting mechanism is usually associated with electron scattering on charged defects in the vicinity of the graphene layer and has been described by the phenomenological relation:

$$\mu = \alpha\frac{N_0}{N}, \quad (2)$$

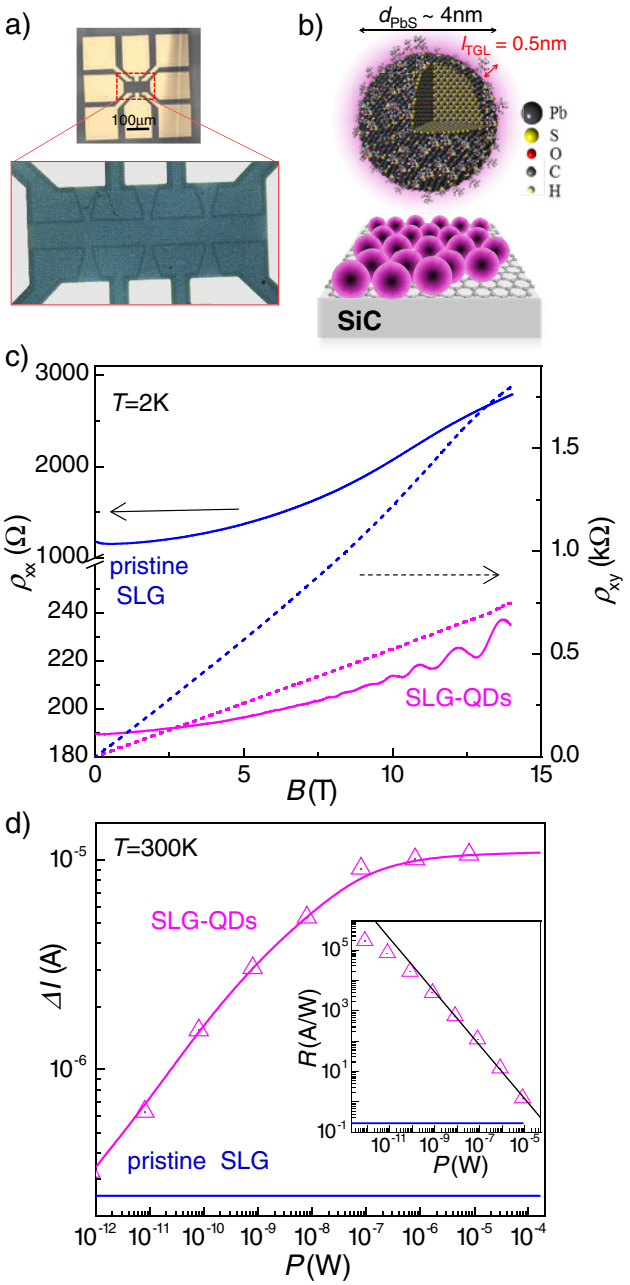

Figure 1. (a) An optical image of a Hall bar device with pristine SiC-grown graphene. (b) A cartoon illustrating the quantum dot structure and the QD deposition on graphene. (c) Longitudinal, ρ_{xx}, (solid lines) and transverse (Hall), ρ_{xy}, (dashed lines) magneto-resistance of the device before and after the QD deposition. (d) Dependence of photocurrent on incident illumination power for pristine SLG and following the QD deposition. Illumination is provided by a laser line $\lambda = 633$ nm, P up to 5 mW mm^{-2}. (Inset) Measured dependence of the photoresponsivity, R, on the incident laser power for the SLG decorated with QDs (triangles). The continuous line describes a power law dependence $R \sim P^{-0.9}$. The blue line describes the noise level.

where N is the concentration of the charged defects, $N_0 = 10^{10}$ cm^{-2} and α is a fitting parameter [22]. These charged defects can include the donor and/or acceptor species that determine the carrier concentration in graphene. Previous studies of the variation of SiC-SLG mobility with electron concentration [11] indicate that relation (2) is valid for SiC-SLG. However, our measured enhancement of both carrier concentration and mobility following the deposition of the QDs is clearly inconsistent with this relation. Furthermore, the model of electrostatic compensation and screening of impurities with opposite charges, previously used to explain the high mobility of CVD p-type SLG decorated with QDs [23] does not apply to our data on SiC-SLG/QD devices since in this case the SLG is n-type.

To explain our findings, we propose a model based on spatial correlation of unipolar, positively charged defects in the QD and the adjacent SiC-SLG layers. We propose that the position of charge within each QD deposited onto graphene is influenced by the Coulomb repulsion by discrete charges near the surface of SiC-SLG; the charge on the QDs would then locate in regions with the lowest electrostatic potential energy. We model the charge distribution numerically by placing

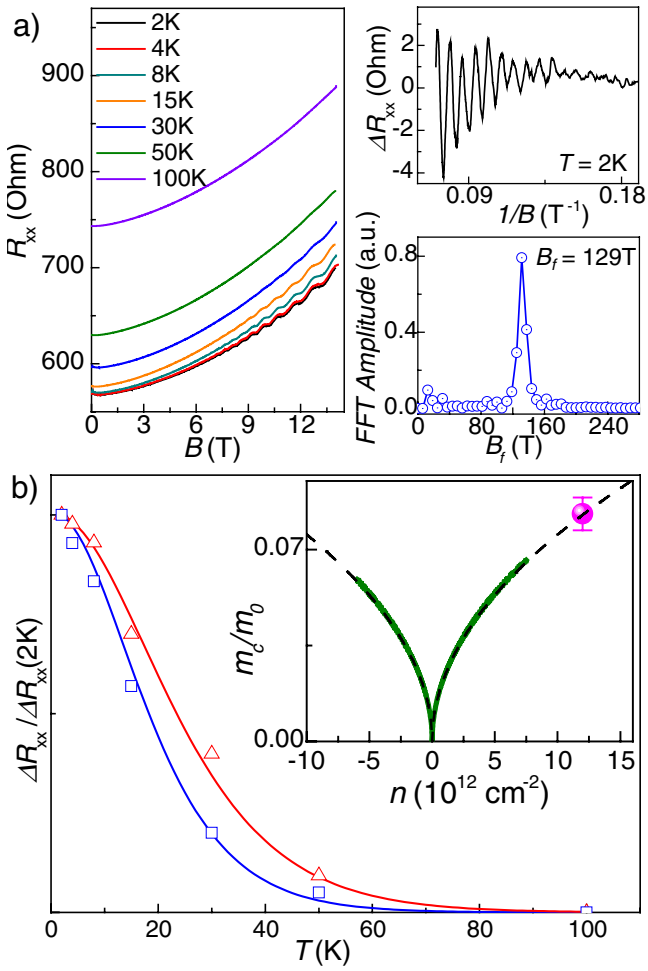

Figure 2. (a) Dependence of R_{xx} on the applied magnetic field in the temperature range 2 K $< T <$ 100 K. Top inset: SdH oscillations at $T = 2$ K after subtraction of parabolic background. Bottom inset: Fourier spectrum of the SdH oscillations ($T = 2$ K) with fundamental magnetic field $B_f = 129$ T. (b) Representative temperature dependence of the SdH amplitude $\Delta R_{xx}(T)/\Delta R_{xx}(2\,\mathrm{K})$ at $B = 13.4$ T (red) and 9.8 T (blue). Fitted lines are obtained with $m_c = 0.083 \pm 0.006\, m_e$. Inset: calculated electron cyclotron mass (data point) compared to the previously published data from [12] (green solid curve). The dashed line is fitted with $v_F = 0.86 \times 10^6$ m s^{-1}.

the charges one by one in the minima of the Coulomb potential (see figure 3 and the supplementary information, SI1 (stacks.iop.org/TDM/4/031001/mmedia)). The charge on the QDs thereby modifies the electrostatic potential landscape created by the randomly distributed charged defects in the SiC layer. The resulting electrostatic potential maps shown in figures 3(b) and (c) for random (uncorrelated) and correlated distributions demonstrate the strong reduction of the amplitude of the potential fluctuations for the case of correlated charges. In the model, we consider the impurity concentration in the SiC/SLG to be equal to the carrier concentration in the pristine graphene, $N_{imp} = n = 5.2 \times 10^{12}$ cm^{-2}. We assume that both impurities and QDs contribute one free electron each to the overall carrier concentration, i.e. $n = N_{imp} + N_{QD} = 12 \times 10^{12}$ cm^{-2}, where the density of QDs is $N_{QD} = 6.8 \times 10^{12}$ cm^{-2}. This value of N_{QD} is in agreement with the estimated areal density assuming tight-packing of QDs with effective diameter $d_{QD} = d_{PbS} + 2l$. Our measurements on the samples with different levels of QD coverage indicate that the deposition of additional layers beyond a monolayer does not influence significantly the device performance. Thus we conclude that efficient charge transfer is predominantly from those QDs in direct contact with the graphene layer and that it is negligibly small between the QDs. Hence only the QD layer adjacent to the SLG makes a significant contribution to the charge correlation.

We find that a random deposition of QDs leads to the increased amplitude of the electrostatic potential fluctuations, calculated as a standard deviation, from $\delta U = 160$ meV (pristine graphene, figure 3(a)) to $\delta U = 250$ meV (graphene and randomly distributed QDs, figure 3(b)). In contrast, for the correlated distribution of QDs, the potential fluctuations are significantly smaller, with $\delta U = 30$ meV (figure 3(c)). Our model therefore supports the conjecture that this reduction of the electrostatic potential fluctuations is responsible for the measured increase of carrier mobility.

We calculate the dependence of the carrier mobility, μ, on impurity density, N_{imp}, for different degrees of spatial correlation of the charges by using

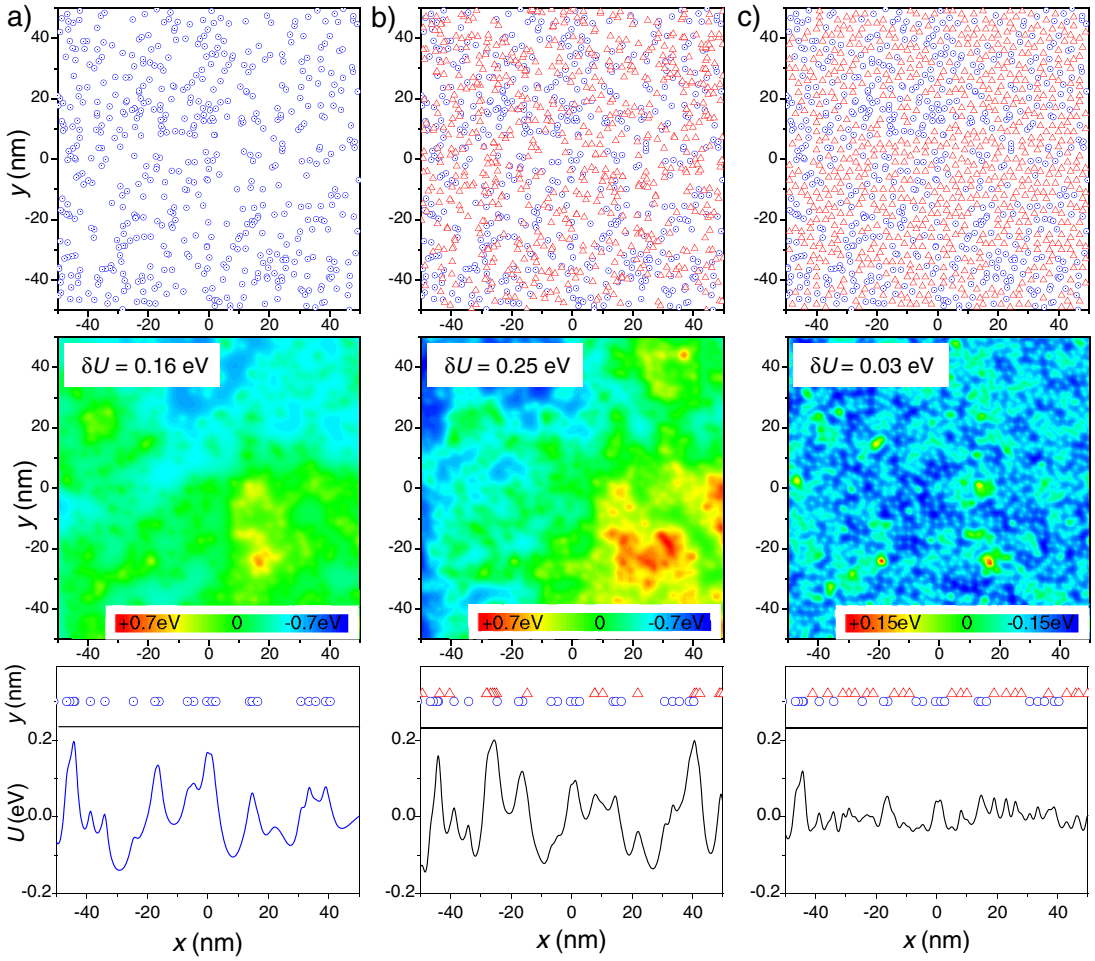

Figure 3. Numerical simulations of the distribution of impurities (blue circles) and charges on QDs (red triangles) top figures, and corresponding local electrostatic potential landscapes (middle figures) for pristine graphene (a), and graphene decorated with QDs that are randomly placed (b) and correlated with potential minima (c). The corresponding change of U describes standard deviation of the potential (bottom figures) for a cross section of the distribution map at $y = 0$.

an analytical model in which the correlation is quantified by the ratio of the maximum to minimum separations between the charged impurities [24]. The maximum distance corresponds to the case when the N_{imp} charges are arranged in an ordered 2D array with the maximum impurity separation, r_i, defined for hexagonal closed-packed (hcp) lattice as $r_i = \sqrt{2}/\sqrt{N_{\mathrm{imp}}\sqrt{3}} \approx 1.1/\sqrt{N_{\mathrm{imp}}}$. Any imperfection in this ordering leads to the reduction of inter-impurity distance, r, in the range $r_0 < r < r_i$, where r_0 is the minimum separation. The degree of correlation of the charged impurities is related to the ratio r_0/r_i, where $r_0/r_i = 1$ corresponds to an ordered distribution, and $r_0/r_i = 0$ to a random distribution. Figure 4(a) shows the results of calculations of mobility versus impurity concentration for $0 < r_0 < 4$ nm. For the uncorrelated case ($r_0 = 0$) the dependence follows equation (2) with $\alpha = 53\ \mathrm{m^2\,V^{-1}\,s^{-1}}$.

For low concentrations, $N_{\mathrm{imp}} < 10^{12}\ \mathrm{cm^{-2}}$, the mobility is almost independent of r_0, indicating that the effect of charge correlation on mobility is negligible in high purity SLG. In this case there is no significant overlap of the electrostatic potentials of the charged impurities and the free carriers always move in a potential due to independent single charges [8]. The model used in [22] considers only charged impurity scattering and does not include other mobility-limiting mechanisms, e.g. phonon scattering [23]. With increasing impurity concentration, the ratio of r_0/r_i increases and when $r_i = 1.1/\sqrt{N_{\mathrm{imp}}}$ approaches r_0, the charged scattering-limited mobility becomes very large, reflecting the absence of scattering in an ordered potential (figure 4(a)).

For the pristine SiC graphene, our experimental values of carrier density and mobility (figure 4(a)) correspond to no correlation ($r_0 = 0$), as in equation (2). The simultaneous increase of both carrier concentration and mobility following deposition of the QD layer cannot be explained by equation (2) (figure 4(a)). However, this result is successfully modelled using our correlated charge model with $r_0/r_i = 0.7$ and $r_0 \approx 2.1$ nm, which is comparable with the nearest neighbour distance estimated for the correlated case in our numerical calculations (figure 3(c) and supplementary information, SI2) and with the radius of our QDs.

To complement our analytical model, we performed Monte Carlo simulations for our unipolar graphene-QD heterostructure. Our model is based on scattering by spatially correlated charges of the same

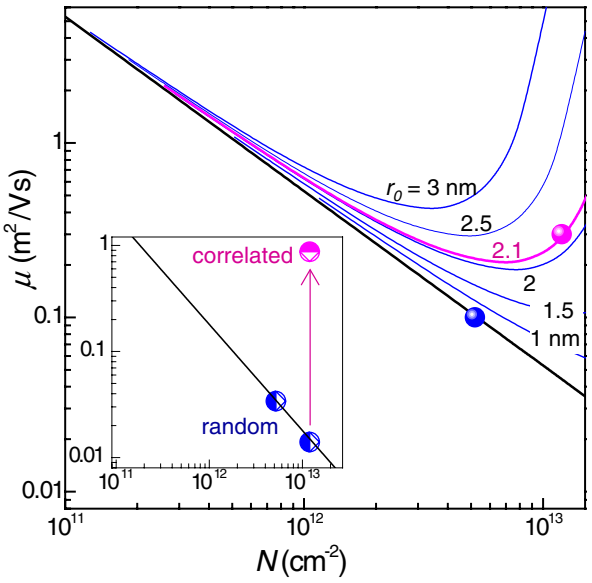

Figure 4. Analytical calculations of the mobility as a function of impurity concentration for different values of the minimum inter-particle distance r_0. Blue and magenta data points represent experimental data for pristine and QD-decorated graphene. The solid line is calculated using equation (2) with $\alpha = 53\ m^2 V^{-1} s^{-1}$. (Inset) Monte-Carlo simulations of electron mobility for the pristine and QD-decorated graphene with and without correlation. The solid line is calculated using equation (2) with $\alpha = 18\ m^2 V^{-1} s^{-1}$.

polarity, i.e. unipolar charges, and excludes charge compensation that would occur in the bipolar case [23]. First, we calculate the carrier mobility for the pristine SiC graphene assuming a random (uncorrelated) distribution of impurities in the SLG (figure 3(a)). The values that we obtain for the mobility are in good agreement with equation (2) with $\alpha = 18\ m^2 V^{-1} s^{-1}$. The discrepancy between the experimental and numerical values of mobility is due to large uncertainties in the value of the phenomenological coefficient α (equation (2)). For the QD-decorated SLG we assume that QDs have a comparable effect on the electron mobility to that of the charged impurities in the SiC (figure 4(b)). The calculation indicates that for $N_{QD} > N_{imp}$, the mobility is determined largely by the degree of spatial correlation of the defect and QD charges. For the case of no correlation (figure 3(b)), we find a conventional decrease of mobility as described by equation (2). In contrast, as shown in figure 3(c), for the case of high correlation of charges, the Monte Carlo simulations indicate that significant increase of mobility is achieved, in good qualitative agreement with our analytical model and with the experimental results (figure 4(a)).

In conclusion, we have measured a significant and simultaneous increase of the photoresponsivity, carrier concentration and mobility in SiC-grown graphene when it is decorated with a layer of colloidal PbS QDs. A unipolar charge correlation model was used to explain our observations. Our numerical calculations indicate that a flattening of the electrostatic potential fluctuations, resulting from the spatial charge correlation, reduces significantly scattering by charged impurities and hence leads to the measured increase of mobility. This conclusion is supported by Monte Carlo simulations of electron transport in our SLG devices. The high carrier concentration and mobility in our devices permits the observation of SdH oscillations and provides an estimate of the electron cyclotron mass in graphene at carrier concentrations up to $1.2 \times 10^{13}\ cm^{-2}$. Our measurements suggest that the decoration of epitaxial graphene with a layer of colloidal QDs or other electrically and optically active capping layers could extend the potential of epitaxial graphene for technological applications.

Acknowledgments

The work is supported by The Leverhulme Trust (grant number RPG-2013-242), the Engineering and Physical Sciences Council (grant number EP/M012700/1), and the EU Graphene Flagship. Authors acknowledge useful discussions with Dr M W Fay and Prof N R Thomas.

Supporting information

Supporting information includes description of the calculations of the electrostatic potential landscape and analysis of 2D charge distribution

Table of content entry

Enhancing optoelectronic properties of SiC-grown graphene by a surface layer of colloidal quantum dots.

Oleg Makarovsky, Lyudmila Turyanska, Nobuya Mori, Mark Greenaway, Laurence Eaves, Amalia Patané, Mark Fromhold, Samuel Lara-Avila, Sergey Kubatkin and Rositsa Yakimova.

A simultaneous increase of carrier concentration, mobility and photoresponsivity is achieved in SiC-grown graphene decorated with colloidal PbS quantum dots, and explained by a unipolar charge-correlation model and Monte Carlo simulations of electron transport. The observation of Shubnikov-de Haas oscillations in these devices provide an estimate of the electron

cyclotron mass in graphene at high electron densities up to 1.2×10^{13} cm^{-2}.

Author contributions

OM and LT performed the experimental studies; NM performed the Monte Carlo simulations; the numerical and analytical modelling was developed by OM, MG and MF. SLA, SK and RY grew the graphene layers and processed the devices. OM, LT, LE and AP analyzed and interpreted the results and co-wrote the manuscript. All authors have contributed to data analysis and approved the manuscript.

References

[1] Ribeiro-Palau R *et al* 2015 *Nat. Nanotechnol.* **10** 965
[2] Janssen T J B M, Tzalenchuk A, Lara-Avila S, Kubatkin S and Fal'ko V I 2013 *Rep. Prog. Phys.* **76** 104501
[3] Nikitskiy I, Goossens S, Kufer D, Lasanta T, Navickaite G, Koppens F H L and Konstantatos G 2016 *Nat. Commun.* **7** 11954
[4] Mudd G W *et al* 2015 *Adv. Mater.* **27** 3760
[5] Li X *et al* 2009 *Science* **324** 1312
[6] Yazdi G R, Iakimov T and Yakimova R 2016 *Crystal* **6** 53
[7] Pallecchi E, Lafont F, Cavaliere V, Schopfer F, Mailly D, Poirier W and Ouerghi A 2014 *Sci. Rep.* **4** 4558
[8] Morozov S. V, Novoselov K. S, Katsnelson M. I, Schedin F, Elias D C, Jaszczak J A and Geim A K 2008 *Phys. Rev. Lett.* **100** 016602
[9] Beshkova M, Hultman L and Yakimova R 2016 *Vacuum* **128** 186
[10] Liu X, Hu T, Miao Y, Ma D, Yang Z, Ma F, Xu K and Chu P K 2016 *Carbon* **104** 233
[11] Tedesco J L, VanMil B L, Myers-Ward R L, McCrate J M, Kitt S A, Campbell P M, Jernigan G G, Culbertson J C, Eddy C R Jr and Gaskill D K 2009 *Appl. Phys. Lett.* **95** 122102
[12] Novoselov K S, Geim A K, Morozov S V, Jiang D, Katsnelson M I, Grigorieva I V, Dubonos S V and Firsov A A 2005 *Nature* **438** 197
[13] Yager T *et al* 2013 *Nano Lett.* **13** 4217
[14] Yager T, Lartsev A, Yakimova R, Lara-Avila S and Kubatkin S 2015 *Carbon* **87** 409
[15] Turyanska L, Patanè A, Henini M, Hennequin B and Thomas N R 2007 *Appl. Phys. Lett.* **90** 101913
[16] Turyanska L *et al* 2015 *Adv. Electron. Mater.* **1** 1500062
[17] Moreels I, Kruschke D, Glas P and Tomm J W 2012 *Opt. Mater. Express* **2** 496
[18] Konstantatos G, Badioli M, Gaudreau L, Osmond J, Bernechea M, Garcia de Arquer F P, Gatti F and Koppens F H L 2012 *Nat. Nanotechnol.* **7** 363
[19] Gusynin V P and Sharapov S G 2005 *Phys. Rev.* B **71** 125124
[20] Witowski A M, Orlita M, Stepniewski R, Wysmołek A, Baranowski J. M, Strupiński W, Faugeras C, Martinez G and Potemski M 2010 *Phys. Rev.* B **82** 165305
[21] Crassee I, Levallois J, Walter A L, Ostler M, Bostwick A, Rotenberg E, Seyller T, van der Marel D and Kuzmenko A B 2011 *Nat. Phys.* **7** 48
[22] Adam S, Hwang E H, Galitski V M. and Das Sarma S 2007 *Proc. Natl Acad. Sci.* **104** 18392
[23] Turyanska L, Makarovsky O, Eaves L, Patanè A and Mori N 2017 *2D Mater.* **4** 025026
[24] Li Q, Hwang E H, Rossi E and Das Sarma S 2011 *Phys. Rev. Lett.* **107** 156601